Nuclear Ccr4-Not mediates the degradation of telomeric and transposon transcripts at chromatin in the *Drosophila* germline

**Maria Kordyukova, Olesya Sokolova, Valeriya Morgunova, Sergei Ryazansky [iD],
Natalia Akulenko, Sergey Glukhov and Alla Kalmykova [iD]***

Institute of Molecular Genetics, Russian Academy of Sciences, Moscow 123182, Russia

ABSTRACT

Ccr4-Not is a highly conserved complex involved in cotranscriptional RNA surveillance pathways in yeast. In *Drosophila*, Ccr4-Not is linked to the translational repression of miRNA targets and the posttranscriptional control of maternal mRNAs during oogenesis and embryonic development. Here, we describe a new role for the Ccr4-Not complex in nuclear RNA metabolism in the *Drosophila* germline. Ccr4 depletion results in the accumulation of transposable and telomeric repeat transcripts in the fraction of chromatin-associated RNA; however, it does not affect small RNA levels or the heterochromatin state of the target loci. Nuclear targets of Ccr4 mainly comprise active full-length transposable elements (TEs) and telomeric and subtelomeric repeats. Moreover, Ccr4-Not foci localize at telomeres in a Piwi-dependent manner, suggesting a functional relationship between these pathways. Indeed, we detected interactions between the components of the Ccr4-Not complex and piRNA machinery, which indicates that these pathways cooperate in the nucleus to recognize and degrade TE transcripts at transcription sites. These data reveal a new layer of transposon control in the germline, which is critical for the maintenance of genome integrity.

INTRODUCTION

The fate of nascent RNA is determined cotranscriptionally by RNA quality control systems. Ccr4-Not is a multicomponent complex found in all studied eukaryotes and is involved in the regulation of gene expression at different stages from transcriptional control to cytoplasmic mRNA degradation (1,2). Ccr4 and Caf1 subunits show deadenylase activity, while the large Not1 subunit serves as a scaffold (3). *Drosophila* Ccr4-Not is the main cytoplasmic complex involved in the deadenylation of mRNAs that determine early development (4–8). Ccr4-Not-mediated mRNA degradation or translational repression is initiated by the recruitment of deadenylase to mRNA 3'UTRs via specific RNA binding proteins (9). Importantly, cytoplasmic Argonaute proteins associate with the Ccr4 deadenylation complex to translationally repress mRNAs. Indeed, Ccr4-Not plays a key role in the translational inactivation of microRNA targets in *Drosophila* and mammals (10–12). In addition, the translational control of distinct maternal mRNAs is mediated by the recruitment of the Ccr4 deadenylation complex through its interaction with the cytoplasmic Piwi subfamily protein, Aubergine (13,14).

In yeast, CCR4-NOT is closely associated with nuclear RNA surveillance and nuclear export (15,16). The nuclear exosome is a multiprotein complex with ribonucleolytic activity that plays an important role in the degradation of aberrant transcripts (17). Nuclear CCR4-NOT associates with the noncanonical Trf4/Air2/Mtr4p polyadenylation (TRAMP) complex and nuclear exosome (16), suggesting that CCR4-NOT may participate in the specific targeting of the degradation machinery in the nucleus. Nuclear CCR4-NOT also displays physical interactions with the components of nuclear export machinery (15,18). This finding is not surprising, since recent data indicate that defects in mRNA 3′-end formation stimulate nuclear exosome activity and affect RNA export efficiency (18–20).

Much less is known about the nuclear functions of the Ccr4-Not complex in higher eukaryotes. Ccr4-Not was recently found in the nuclei of *Drosophila* ovarian cells (21), suggesting its yet undiscovered role in nuclear RNA surveillance.

Ccr4-Not components were identified among the factors involved in telomeric retrotransposon *HeT-A* silencing in the *Drosophila* germline (21,22). The depletion of Ccr4 caused the accumulation of *HeT-A* transcripts in germ cells, accompanied by the elongation of the *HeT-A* poly(A) tail (21). Surprisingly, the observed effect was germline-specific, suggesting a particular role for Ccr4-Not in germ cells. In

the germline, the expression of transposable elements (TEs), including telomeric retroelement *HeT-A,* is also regulated by the Piwi-interacting RNA (piRNA) pathway (23,24). Ccr4 and mRNA degradation enzymes have been implicated as responsible for the removal of retroelement transcripts in the cytoplasm of germ cells (22), although the link between mRNA degradation and piRNA pathways has not been established. In the present study, by examining the mechanism of Ccr4-mediated *HeT-A* silencing, we revealed the functional relationship between different nuclear RNA silencing pathways in the germline.

The piRNA pathway operates in the gonads of animals to protect their genomes from the expansion of TEs (25). Transposon-specific piRNAs are derived from piRNA precursor transcripts originating from dedicated genomic sources called piRNA clusters. *Drosophila* and other arthropod species have evolved a sophisticated mechanism allowing piRNA production from heterochromatic loci enriched by TE remnants (26). In contrast, in the mammalian prenatal germline, most piRNA clusters that give rise to primary piRNAs are represented by individual transposons (27). In *Drosophila*, piRNA clusters associated with recently transposed TEs were also discovered (28), suggesting an evolutionarily conserved origin of anti-transposon piRNAs. A hallmark of *Drosophila* TE-associated piRNA clusters is the production of flanking piRNAs from opposing genomic strands upstream and downstream of the TE insertions (28,29).

In flies, dual-strand piRNA clusters that produce piRNA precursors from both genomic strands play an essential role in anti-transposon control (24). These piRNA clusters have a specific chromatin structure enriched by trimethylated lysine 9 histone H3 (H3K9me3), which is recognized by Rhino (Rhi), the germline-specific ortholog of heterochromatin protein 1 (HP1) (30–32). Similar to heterochromatic piRNA clusters, standalone active TEs producing piRNAs also associate with H3K9me3 and Rhi (31). Specific chromatin components of dual-strand piRNA clusters mediate the transcription of long piRNA precursors and their export from the nucleus (33–38). The post-transcriptional cleavage of piRNA cluster and TE transcripts accompanied by piRNA generation is exerted in the cytoplasm by endonuclease Zucchini and by Ago3/Aubergine Piwi-subfamily proteins implemented in the ping-pong piRNA amplification cycle (24,39–41). piRNAs guide TE silencing; transcriptional gene silencing (TGS) is considered the main mechanism of the piRNA-mediated downregulation of TE expression (42,43). Indeed, in somatic follicular cells, nuclear Piwi protein acts mainly through TGS because a strict correspondence was observed between TE expression changes in nascent and steady-state RNA levels upon *piwi* knockdown in follicular cells. However, significantly greater changes were observed in steady-state transposon RNA levels than in nascent transcript abundance upon germline *piwi* knockdown, suggesting strong post-transcriptional effects of Piwi loss (42). The nature of this presumed mechanism of post-transcriptional transposon silencing remains unclear. In addition, statistical analysis revealed a lack of a relationship between piRNA abundance and transpositional activity for TE families (44), suggesting that active TEs should be silenced by an additional mechanism.

The yeast model clearly shows that the repression of heterochromatic genes does not occur exclusively at the transcriptional level. Transcripts emerging from heterochromatin are channeled into the nuclear RNA decay pathway for degradation at the site of transcription, a process referred to as cotranscriptional gene silencing (CTGS) (45,46). CTGS in both fission and budding yeasts depends on a specialized polyadenylation complex, TRAMP, which likely targets heterochromatic transcripts for degradation by the exosome—the main RNA degradation complex in the nucleus (47,48).

Our data fill a gap in the understanding of TE control mechanisms in the germline. We found that nuclear Ccr4-Not complex cotranscriptionally recognizes TE transcripts to promote their degradation. Interactions with the components of the piRNA system may define the Ccr4-Not targets in *Drosophila* ovaries. Our data indicate that the germline-specific nuclear functions of the *Drosophila* deadenylase Ccr4-Not complex involve the repression of especially dangerous active TEs as well as the nuclear biogenesis of telomeric transcripts.

MATERIALS AND METHODS

Drosophila melanogaster strains

We used the following *twin* alleles: *twin^{S1}* (Bloomington Drosophila Stock Center (BDSC) 32553) and *twin^{S3}* (BDSC 32554) point mutations; P{wHy}twin^{DG24102} (BDSC #21238) insertion-associated allele; chromosomal deletion affecting *twin* Df(3R)crb87-4 (BDSC #2362). GLKD (GermLine KnockDown) flies were the F1 progeny from the cross of two strains bearing constructs with short hairpin (sh) RNA (spnE_sh, #103913, VDRC; piwi_sh, #101658, VDRC; twin_sh, #32490, BDSC and white_sh, #33623, BDSC) and strain *P{UAS-Dcr-2.D}1, w^{1118}, P{GAL4-nos.NGT}40*, #25751 BDSC, providing GAL4 expression under the control of the germline-specific promoter of the *nanos (nos)* gene. Strains expressing pUASp-EGFP-Cuff (38), Piwi-GFP (49) and UASp-Ccr4-HA (50) were used. *y^1 w^{67c23}* (*yw*) laboratory strain was used as a control. We used *piwi^2* and *piwi^{Nt}* alleles (51). *spindle-E* (*spnE*) mutations were *spn-E^{616}* and *spn-E^{hls3987}*.

RT-PCR, nuclear run-on (NRO) transcription and RNA *in situ* hybridization

RNA was isolated from the ovaries of 3-day-old females. The cDNA was synthesized using random hexamers and SuperScriptII reverse transcriptase (Life Technologies). The cDNA samples were analyzed by real-time quantitative polymerase chain reaction (PCR) using SYTO-13 dye on a LightCycler96 (Roche). The values were averaged and normalized to the expression level of the ribosomal protein gene *rp49*. NRO transcription was performed as previously described (52). The primers used are listed in Supplementary Table S4. *In situ* RNA analysis was performed according to a previously described procedure (53) using digoxigenin (DIG)-labeled strand-specific riboprobe and anti-DIG antibodies conjugated with alkaline phosphatase (Roche) or FITC (Roche). The probe corresponding to 2L-3L TAS was a cloned PCR fragment obtained using the

primers listed in Supplementary Table S4. Antisense *HeT-A* riboprobe containing a fragment of the ORF (nucleotides 4330–4690 of GenBank sequence DMU06920) was used.

Genome sequencing and prediction of TEs

Single-end libraries of genomic DNA from females of the *twin* ^{DG24102}/*Df(3R)crb87-4* strain were prepared according to the Illumina standard protocol and sequenced on the Illumina HiSeq 1500 platform. TE insertion sites were predicted by using the McClintock meta-pipeline (https://github.com/bergmanlab/mcclintock) with the canonical sequences of TEs (http://www.fruitfly.org/p_disrupt/TE.html) and the annotated TE insertion sites in the reference *iso-1* strain (FlyBase, r.6.13).

Chromatin-associated and small RNA library preparation and analysis

Chromatin-associated RNA was prepared from the ovaries of transheterozygous *twin* ^{DG24102}/*Df* and heterozygous *twin* mutants according to a previously published procedure (34). The cDNA was synthesized using the SuperScript Double-Stranded cDNA Synthesis Kit (Invitrogen). The tagmentation reaction was performed according to a previously published protocol (54) using in-house produced Tn5 charged with oligonucleotides compatible with the Illumina system. The reaction products were cleaned using a cleanup mini kit (Evrogen), PCR amplified and sequenced on the Illumina HiSeq1500. After removing the Illumina 3′ adapter, the rRNA reads were filtered out, and the remaining reads were mapped to the genome assembly of *Drosophila melanogaster* (BDGP assembly R6/dm6) by bowtie2 (55).

The abundance of genic chromatin-associated transcripts was counted by overlapping the single-mapped Chrom-seq reads with protein-encoding gene bodies according to the dm6 gene annotation scheme from Illumina iGenome by featureCount. A gene was removed from the analysis if it contained a TE insertion or was located near a TE (≤ 5 kb). Annotated (FlyBase, r.6.13) and predicted TE copies were considered. Transposon- and piRNA cluster-derived chromatin-associated transcripts were revealed by mapping to the canonical sequences of TEs (http://www.fruitfly.org/p_disrupt/TE.html) or to the piRNA clusters (24) by bowtie2. The quantification of chromRNA-seq reads corresponding to TEs (Supplementary Table S1) was performed by overlapping the single-mapped reads with the annotated TE copies (FlyBase, r.6.13) by bedTools. Only standalone TE copies that did not overlap gene, tRNA, miRNA, rRNA or snRNA loci were used for the analysis. TE was considered full-size if its length was at least 90% of the length of the canonical consensus sequence (https://github.com/bergmanlab/transposons/blob/master/releases/transposon_sequence_set_v9.42.embl.txt); otherwise, the TE was classified as a truncated sequence.

Small RNAs (19–29 nt) from total ovarian RNA extracts of *twin* mutants were cloned as previously described (56). The libraries were barcoded according to the instructions of the Illumina TruSeq Small RNA Sample Prep Kit

and submitted for sequencing using the Illumina HiSeq-2500 sequencing system. Ovarian small RNAs from *twin* ^{DG24102}/*Df(3R)crb87-4* were sequenced as two technical replicates that were subsequently merged for the analysis. After clipping the Illumina 3′ adapter sequence, small RNA reads that passed quality control and minimal length filter (>18 nt) were mapped (allowing 0 mismatches) to the *D. melanogaster* genome (BDGP assembly R6/dm6) by bowtie2. To identify piRNAs derived from TEs and piRNA clusters, small RNA reads were mapped to the canonical sequences of TEs (http://www.fruitfly.org/p_disrupt/TE.html) or to the piRNA clusters (24) by bowtie2. The calculation of piRNAs derived from TE flanking regions was performed as previously described (28). The quantification of small RNA reads corresponding to TEs (Supplementary Table S1) was performed by overlapping the single-mapped reads with the annotated TE copies (FlyBase, r.6.13) by bedTools. Genic piRNAs were counted by overlapping the single-mapped 23–29 nt reads with gene bodies according to the dm6 gene annotation scheme from Illumina iGenome by featureCount.

Chromatin immunoprecipitation

ChIP was performed according to a published procedure (57). Chromatin was immunoprecipitated with the following antibodies: anti-HP1a (C1A9 Developmental Studies Hybridoma Bank), anti-trimethyl-histone H3 Lys9 (Abcam) and Rhi antiserum (58). The primers used in this study are listed in Supplementary Table S4. Quantitative PCR was conducted with a Light cycler 96 (Roche). The obtained values were normalized to input and compared with values for the *rp49* gene as a control genomic region. ChIP using dual cross-linking with ethylene glycol bis(succinimidyl succinate) (EGS) and formaldehyde (59) was performed to improve the detection of Ccr4-HA or Not1 by ChIP. Standard error of mean (SEM) of triplicate PCR measurements for three biological replicates was calculated.

DNA FISH and immunostaining

The combination of protein and DNA localization was performed according to a previously described procedure (60). The *HeT-A* probe used for DNA FISH was a cloned fragment of the *HeT-A* ORF (61). The probe corresponding to 2R-3R TAS was a cloned PCR fragment obtained using the primers listed in Supplementary Table S4. The probes were labeled using a DIG DNA labeling kit (Roche). Rat anti-Rhi antibodies (58) were used. To stain the DNA, the ovaries were incubated in PBS containing 0.5 µg/ml 4',6-diamidino-2-phenylindole (DAPI). Two biological replicates were obtained for each experiment. The Zeiss LSM 510 Meta confocal microscope was used for visualization. Confocal image z-stacks generated with the slice step of 1.5 µM were used for the statistics.

Immunostaining was carried out according to the previously described procedure (62). The following primary antibodies were used for immunostaining: mouse anti-Not1 (6) (kindly provided by E. Wahle), rat anti-HOAP (polyclonal

antibodies against full-length HOAP protein were generated by the Immunochemistry laboratory, Branch of IBC RAS, Pushchino, Russia), guinea pig anti-HipHop (kindly provided by Y. Rong), rabbit anti-Ccr4 (6) (kindly provided by M. Simonelig), mouse anti-Piwi (kindly provided by J. Brennecke), anti-GFP (Abcam).

Coimmunoprecipitation (co-IP) of nuclear protein complexes

Four hundred pairs of ovaries were dissected per one sample. Nuclei were isolated as described previously (52), washed with HDG150 buffer (20 mM HEPES (pH 7.9), 150 mM NaCl, 10% glycerol, 20 mM NaF, 0.2 mM NaVO$_4$, Complete mini protease inhibitor cocktail (Roche)) and pelleted by centrifugation at 1700 *g* for 10 min at 4°C. Then five volumes of High Salt buffer (20 mM HEPES (pH 7.9), 300 mM NaCl, 1.5 mM MgCl$_2$. 0.2 mM ethylenediaminetetraacetic acid (EDTA), 0.3% NP-40, 10% glycerol, 20 mM NaF, 0.2 mM NaVO$_4$, Complete mini protease inhibitor cocktail (Roche)) were added to the nuclei and the samples were incubated on a rotator for 15 min at room temperature (RT). Afterward, the equal volume of Low salt buffer (20 mM HEPES (pH 7.9), 1.5 mM MgCl$_2$. 0.2 mM EDTA, 10% glycerol, 20 mM NaF, 0.2 mM NaVO$_4$, Complete mini protease inhibitor cocktail (Roche)), 0.1 U/ul bensonase (Sigma)) was added and the samples were incubated with rotation for 15 min at RT. Next, the lysates were cleared by centrifugation at 16 000 *g* for 10 min at 4°C. For coimmunoprecipitation (co-IP) experiments, the lysates were mixed either with the non-immobilized primary antibodies or anti-HA-conjugated beads (20 μl, Pierce) and incubated on a rotator for 30 min at RT. Protein-G or Protein-A Dynabeads (50 μl, Thermo Fisher Scientific) were added to the co-IP samples pre-incubated with mouse or rabbit primary antibodies, respectively, and additionally incubated on a rotator for 15 min at RT. Before the experiment, all types of the beads were preincubated with 2 mg/ml bovine serum albumin in HDG150 buffer on a rotator overnight at 4°C and washed three times with HDG150 buffer. After the immobilization of immune complexes, the beads were washed with HDG150 three times with rotation for 5 min at RT. The elution was performed with 100 μl Laemmli protein loading buffer (25 mM Tris–HCl, pH 6.8, 10% glycerol, 1% SDS, 0.005% bromophenol blue, 2.5% β-mercaptoethanol) at 100°C for 5 min. Samples were resolved by 8% sodium dodecyl sulphate-polyacrylamide gelelectrophoresis (SDS-PAGE) and transferred onto PVDF membrane Immobilon-P (Millipore) or Protran nitrocellulose membrane (Amersham). Blots were developed using the Immun-Star AP detection system (Bio-Rad Laboratories), in accordance with the manufacturer's recommendations. Fractionation of ovaries was verified by western blotting using following antibodies: anti-γ-tubulin (Sigma), anti-HP1a (C1A9, Developmental Studies Hybridoma Bank), Egl antiserum (rat polyclonal antibodies against Egl fragment (amino acids 1–467) were generated by the Immunochemistry laboratory, Branch of IBC RAS, Pushchino, Russia). For co-IP experiments and western blotting the following antibodies were used: anti-Not1 (6), anti -Ccr4 (6), anti-GFP (Abcam), normal mouse IgG (Santa Cruz Biotechnology), normal rabbit

IgG (Santa Cruz Biotechnology), anti-HA (Cell Signaling Technology, 6E2), anti-Piwi (24), anti-Thoc5 (63).

RESULTS

Ccr4 depletion causes the accumulation of full-length TE transcripts in the chromatin-associated RNA fraction in the germline

In a previous study, we showed that the depletion of the Ccr4-Not components led to the overexpression of the telomeric retrotransposon *HeT-A* in the germline but not in somatic tissues (21). Ccr4-Not components are associated with the chromatin fraction in *Drosophila* ovaries (21), suggesting a nuclear role for Ccr4-Not in the germline. In this study, we address the nuclear function of the Ccr4-Not deadenylase complex in the *Drosophila* female germline.

Mutant alleles of *twin* encoding Ccr4 cause severe ovarian defects (5), which limits their application in some experiments. In this study, we use the hypomorphic allele *twin*^{DG24102} (64) and germline knockdown (GLKD) of *twin* that exert a similar effect on *HeT-A* expression (21). In both cases, ovaries were reduced but suitable for analysis.

Using RNA FISH on the ovaries of *twin*_GLKD, we revealed abundant *HeT-A* transcripts in the nucleus and cytoplasm of nurse cells and oocytes (Figure 1A). In nurse cell nuclei, *HeT-A* transcripts accumulated near telomeres stained for the telomere-specific protein HOAP (65) (Figure 1B). Nurse cells are highly polyploid, but their chromatids are only partially conjugated. Thus, we observed much more HOAP signals than the number of chromosome arms. Using three-dimensional (3D) confocal images of the nurse cell nuclei for the quantification, we have revealed 50 ± 5 (mean ± standard deviation, SD) HOAP signals in every nucleus ($n = 12$), but only 11 ± 3 of them are associated with *HeT-A* RNA spots. This fact may be explained by the various *HeT-A* copy numbers in different telomeres. Alternatively, *HeT-A* transcripts arising from different telomeres may have different fates. Thus, two populations of *HeT-A* RNA are revealed upon *twin* depletion, in the cytoplasm and near transcription sites at telomeres.

To characterize the changes in the nuclear RNA caused by Ccr4 depletion, we performed chromatin-bound RNA-seq (chromRNAseq) from the ovaries of heterozygous and transheterozygous *twin* mutants in replicates. This RNA fraction is enriched in unprocessed nascent RNAs (Figure 1C; Supplementary Figures S1 and 2) similar to nuclear run-on RNAs (66). To annotate chromRNAseq data, we subdivided TEs into several groups. *HeT-A*, *TART* and *TAHRE* were considered as telomeric TEs. Non-telomeric piRNA clusters were those described in (24) except for the telomeric and subtelomeric regions. Standalone euchromatic TEs are defined according to Flybase r.6.13 as located in euchromatin and not belonging to the annotated piRNAs clusters (24). The annotation of chromRNAseq data has shown the accumulation of euchromatic and telomeric TE transcripts in *twin* mutants, while non-telomeric piRNA cluster transcripts were unaffected (Figure 1D). Next, we mapped chromatin RNAseq data to all annotated for the sequenced *D. melanogaster* genome TE insertions.
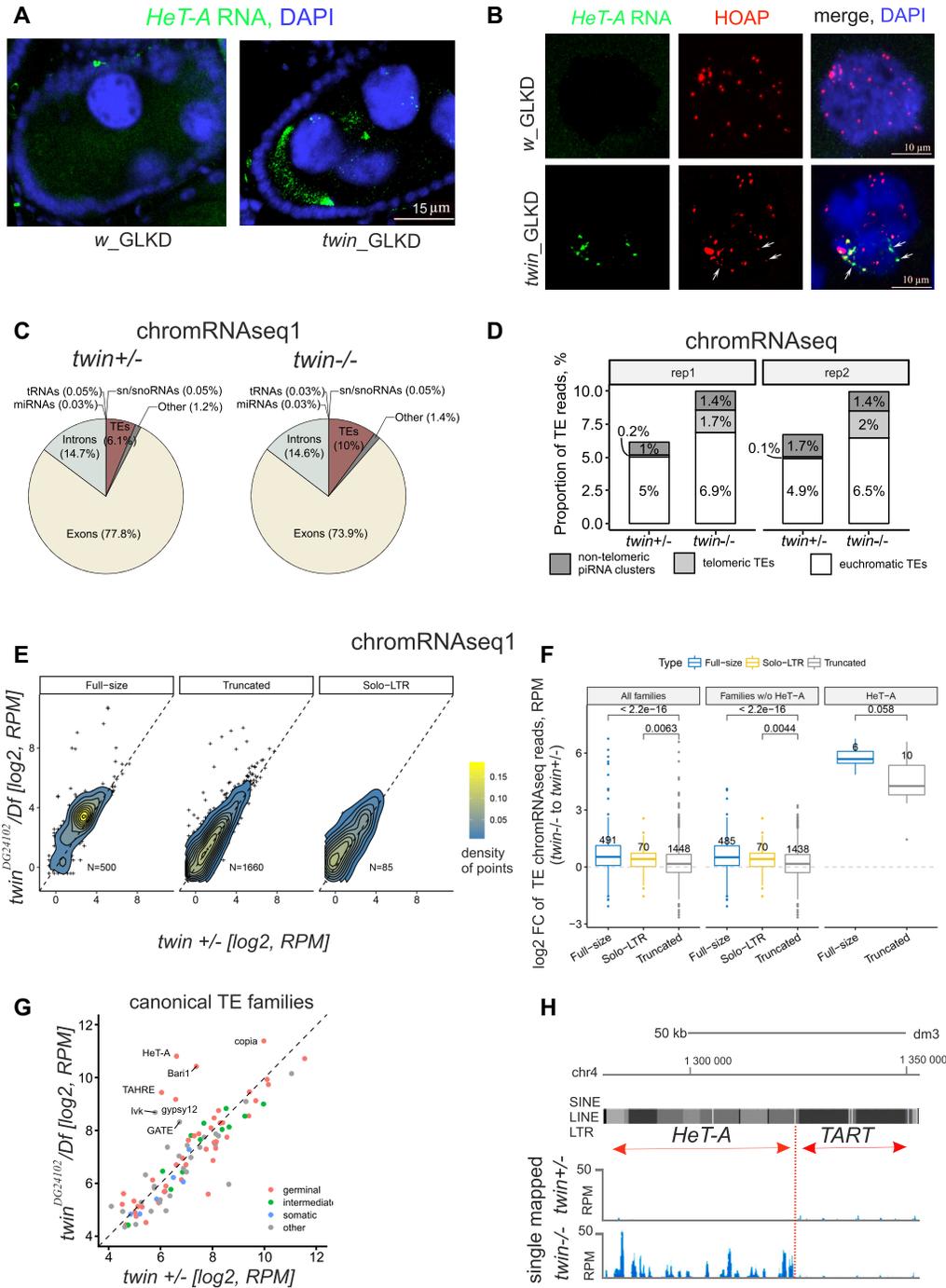
Figure 1. Ccr4 depletion causes the accumulation of active TE transcripts in the ovarian chromatin-associated RNA fraction. (**A**) *HeT-A* RNA FISH (green) in the germline in wild type background and upon *twin*_GLKD. Egg chambers at stage V-VII of oogenesis are shown. (**B**) *HeT-A* transcripts associate with telomeres in *twin*_GLKD (arrows). *HeT-A* RNA FISH (green) combined with immunostaining of telomeric protein HOAP (red) was performed on *Drosophila* ovaries upon *w*_GLKD and *twin*_GLKD. (**C**) Pie diagram showing the annotation of transcripts in chromatin-bound RNA fractions from *twin+/-* and *twin-/-* mutants. (**D**) Proportions of chromRNAseq reads corresponding to indicated TE groups in *twin* mutants. Data for two chromRNAseq replicas are shown. (**E**) Scatter plots of log2-transformed and RPM-normalized chromatin RNAseq1 reads in the ovaries of heterozygous and transheterozygous Ccr4 mutants mapped to the full-length and partial genomic TE copies and solo-LTRs. The scatterplots were additionally smoothed to show the density of points; outlier points are shown as plus-signs. Color bars depict the point densities on the plots. The numbers of full-length TEs, partial TEs and solo-LTRs used for the construction of plots are indicated. (**F**) Boxplots demonstrating a correlation between TE length and upregulation in Ccr4 mutants (Wilcoxon test). Most of the Ccr4 TE targets are full-length copies. (**G**) Scatter plot of log2-transformed and RPM-normalized chromatin RNAseq1 reads in the ovaries of heterozygous and transheterozygous Ccr4 mutants mapped to canonical sequences of TE families. The color of the dots indicates the type of TEs according to their transcription patterns in ovaries (73). (**H**) Accumulation of telomeric transcripts in the chromatin-bound RNA fraction in *twin* mutants. The picture is generated using the UCSC Genome Browser. Chromatin RNAseq reads are shown in RPM. The genomic coordinates are indicated (dm6).

TEs were subdivided into three types: full-length and partial TE copies and solo-LTRs (long terminal repeats) (Figure 1E). This analysis revealed that the most sensitive TE targets of Ccr4 are full-length TE copies. Indeed, the degree of TE upregulation in Ccr4 mutants strongly correlates with their length: there are significantly more full-length TE copies among Ccr4 targets (Figure 1F and Supplementary Figure S2). We generated a list of all annotated TE copies affected by Ccr4 mutations, setting a cutoff of 1.0 (log2 chromRNA fold changes), and revealed the upregulation of many TE copies related to various families (Supplementary Table S1). The mapping of chromatin RNAseq data to a canonical set of TEs revealed the most sensitive TE families, such as telomeric elements *HeT-A* and *TAHRE, copia, Bari1, GATE, Ivk* and *gypsy12* (Figure 1G, Supplementary Figure S2). Interestingly, in contrast to *HeT-A*, expression of the telomeric retroelement *TART* is not affected by Ccr4 (Figure 1H). We suggested that the most sensitive TE families contain a higher proportion of full-length copies. Indeed, *copia* and *Bari1* TE families predominantly consist of full-length copies in the sequenced *D. melanogaster* genome (67). However, this explanation is not consistent with the finding that *Ivk* and *GATE* are predominantly represented by partial copies (67). Indeed, the proportion of full-length elements does not determine the differential response of TE families to Ccr4 depletion (Supplementary Table S2). The selectivity of Ccr4 to particular TE families is likely determined by the regulatory peculiarities or genomic context of TE insertions.

Thus, the Ccr4-Not complex regulates the RNA levels of full-length and, therefore, active TEs. *HeT-A* and *TAHRE* are not exceptions because their promoters located in the 3′ UTR remain intact, even in the 5′ truncated copies (58,68,69).

The transcripts of subtelomeric repeats, TAS (telomere-associated sequences), were also accumulated in the chromatin-bound RNA fraction in Ccr4 mutants (Figure 2A). Using *in situ* RNA hybridization, we detected increased levels of TAS transcripts in nurse cell nuclei upon *twin*_GLKD, similar to the results observed in ovaries with a depleted piRNA pathway (Figure 2B). Telomeric retrotransposon arrays and TASs constitute specific telomeric Rhi-dependent piRNA clusters that require piRNAs for the maintenance of their chromatin state in the germline (70). Notably, the levels of the telomeric piRNA cluster transcripts are downregulated by Ccr4 in the chromatin-bound RNA fraction; however, Ccr4-Not does not play a role in the expression of nontelomeric germline piRNA clusters (Figure 2C and Supplementary Figure S2). Interestingly, although expression of nontelomeric piRNA clusters is generally not affected by Ccr4 depletion, particular TEs located within *42AB* and *80F* clusters are upregulated in Ccr4 mutants (Figure 2D). These TEs are most likely transcriptionally active copies.

Next, we explored whether the Ccr4 mutation affects the levels of RNAs derived from protein-encoding genes. The genes located in close vicinity of TEs (≤5 kb) were excluded from this analysis. Setting a cutoff of 1.5 (log2 chromRNA fold changes), we generated a rather short list of Ccr4-dependent genes (Supplementary Table S3), suggesting that in general, nuclear Ccr4 is dispensable for coding gene reg-

ulation in the germline. Exploring the genome browser, we revealed that most of the Ccr4 target genes are grouped into two large genomic loci containing full-length TE insertions among the genes (Figure 2E and Supplementary Table S3). First, we observed that these genes are not expressed in wild-type ovaries. The accumulation of transcripts derived from these loci is observed in Ccr4 mutants. We suggest that Ccr4 could play a role in the degradation of long spurious transcripts generated as a result of TE read-through transcription. These transcripts are degraded in wild-type ovaries and become visible only after the depletion of Ccr4.

Notably, the abundance of chromatin-bound *nos, hsp70* and *CycA* transcripts that are regulated by Ccr4-mediated cytoplasmic deadenylation (5,7,8) is not affected by *twin* mutations (Supplementary Figure S3), suggesting distinct roles for nuclear and cytoplasmic Ccr4 complexes in the germline.

Ccr4 depletion causes the accumulation of TE transcripts in chromatin but does not affect the transcription state of transposons

To explore the mechanism of Ccr4-mediated silencing, we compared TE and piRNA cluster expression in different ovarian RNA fractions upon Ccr4 depletion (Figure 3A). TE and piRNA cluster RNA levels were estimated by RT-qPCR in total, nuclear run-on (NRO) and chromatin-associated ovarian RNA samples upon *twin*_GLKD. The NRO RNA fraction reflects the levels of nascent transcript synthesis (71). *HeT-A, GATE, copia* and *Bari1* were upregulated upon *twin*_GLKD; their transcripts accumulate in chromatin-bound but not in NRO RNA samples, suggesting a fundamental difference between these RNA fractions. *Piwi*_GLKD led to the transcriptional derepression of *HeT-A, GATE* and *copia,* indicating that these elements are regulated at both the transcriptional and cotranscriptional levels. Interestingly, the repression of the Tc1-like transposon *Bari1* occurs predominantly at the cotranscriptional level, while *TART-A* and *HMS Beagle* are silenced at the transcriptional level (Figure 3A). We failed to detect changes in the expression of the nontelomeric piRNA clusters upon *twin*_GLKD, similar to the results obtained with Ccr4 mutants. Thus, specific silencing pathways control the expression of different TE families, which most likely depends on the peculiarities of their regulatory elements and binding proteins.

In human cells, a fraction of telomeric repeat-containing RNA (TERRA) remains telomere-associated after its transcription (72). Comparison of the *HeT-A* transcript abundance normalized to *rp49* housekeeping gene RNA in total and chromatin ovarian RNA fractions shows the accumulation of *HeT-A* transcripts near chromatin in wild-type ovaries. However, Ccr4 depletion modestly affects *HeT-A* RNA retention at chromatin (Figure 3B), suggesting that an unknown mechanism provides the retention of *HeT-A* RNA at telomeres even under strong *HeT-A* overexpression.

Taken together, these data indicate that nuclear Ccr4-Not function is required for the cotranscriptional degradation of *HeT-A* and other TE RNA in the germline.
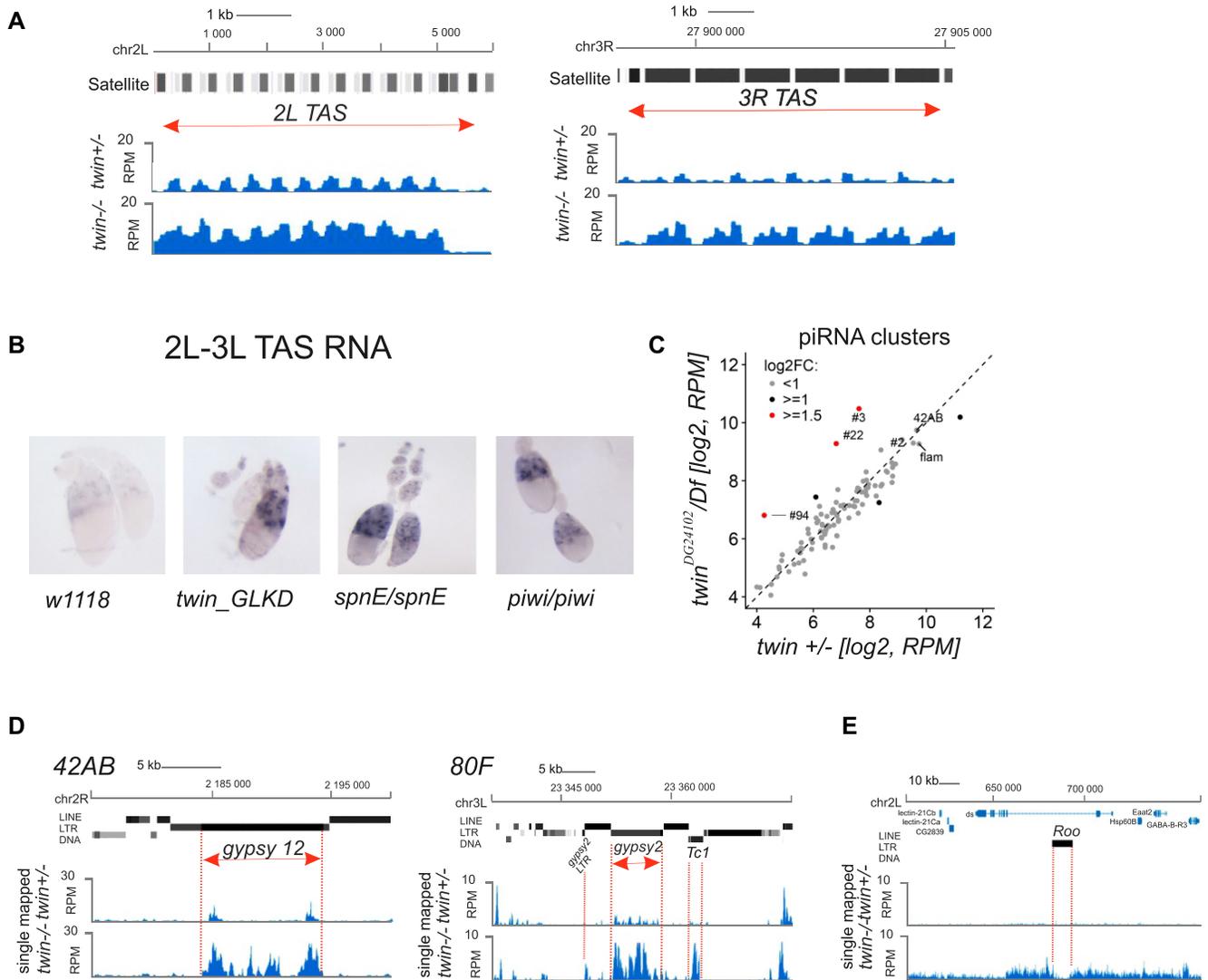
Figure 2. Ccr4 depletion causes the accumulation of subtelomeric transcripts near telomeres but does not affect nontelomeric germline piRNA clusters. (**A**) Accumulation of subtelomeric transcripts in the chromatin-bound RNA fraction in *twin* mutants. The picture was generated using the UCSC Genome Browser. (**B**) *In situ* RNA hybridization of the 2L-3L TAS probe with ovaries of the indicated genotypes. (**C**) Scatter plot of chromatin RNAseq reads mapped to piRNA clusters (24). #3, #22 and #94 are telomeric piRNA clusters. (**D**) Chromatin-associated RNAs from piRNA clusters. The fragments of the *42AB* and *80F* dual-strand piRNA clusters containing both upregulated and non-affected TEs are shown. (**E**) Chromatin-RNAseq reads mapping to the genomic locus at region *21E* are shown. The pictures (D and E) were generated using the UCSC Genome Browser. Dotted lines indicate the borders of the TEs.

ChromRNAseq data clearly demonstrated that the targets of Ccr4-Not in the germline are TEs and telomeric repeats, the expression of which is regulated by the piRNA system, promoting the hypothesis that Ccr4-Not and piRNAs could act in the same silencing pathway. To test this idea, we performed a double-knockdown test. We constructed a strain depleted of the germline protein Ccr4 (*twin*_GLKD) and the RNA helicase Spindle-E (*spnE*_GLKD), which is involved in the piRNA pathway (73,74). RT-qPCR analysis of *HeT-A* steady-state RNA levels in the ovaries shows that there is no additive effect of double knockdowns relative to *spnE*_GLKD, suggesting that Ccr4 and SpnE act in the same pathway, at least in the *HeT-A* expression control (Figure 3C). This result was confirmed by *HeT-A* RNA *in situ* hybridization using single and double *spnE;twin* or *piwi;twin* GLKD (Supplementary Figure S4). These data indicate that Ccr4 may act together with the piRNA pathway to silence *HeT-A* telomeric repeats.

The Ccr4-Not complex is located near chromatin but does not affect the chromatin state of its targets

To address the nuclear localization of Ccr4-Not in the ovary, we performed ovary immunostaining. The diffuse cytoplasmic distribution of Ccr4-Not in ovarian cells was previously reported (8,14,64). To reveal nuclear Ccr4-Not, we applied an approach based on more profound permeabiliza-
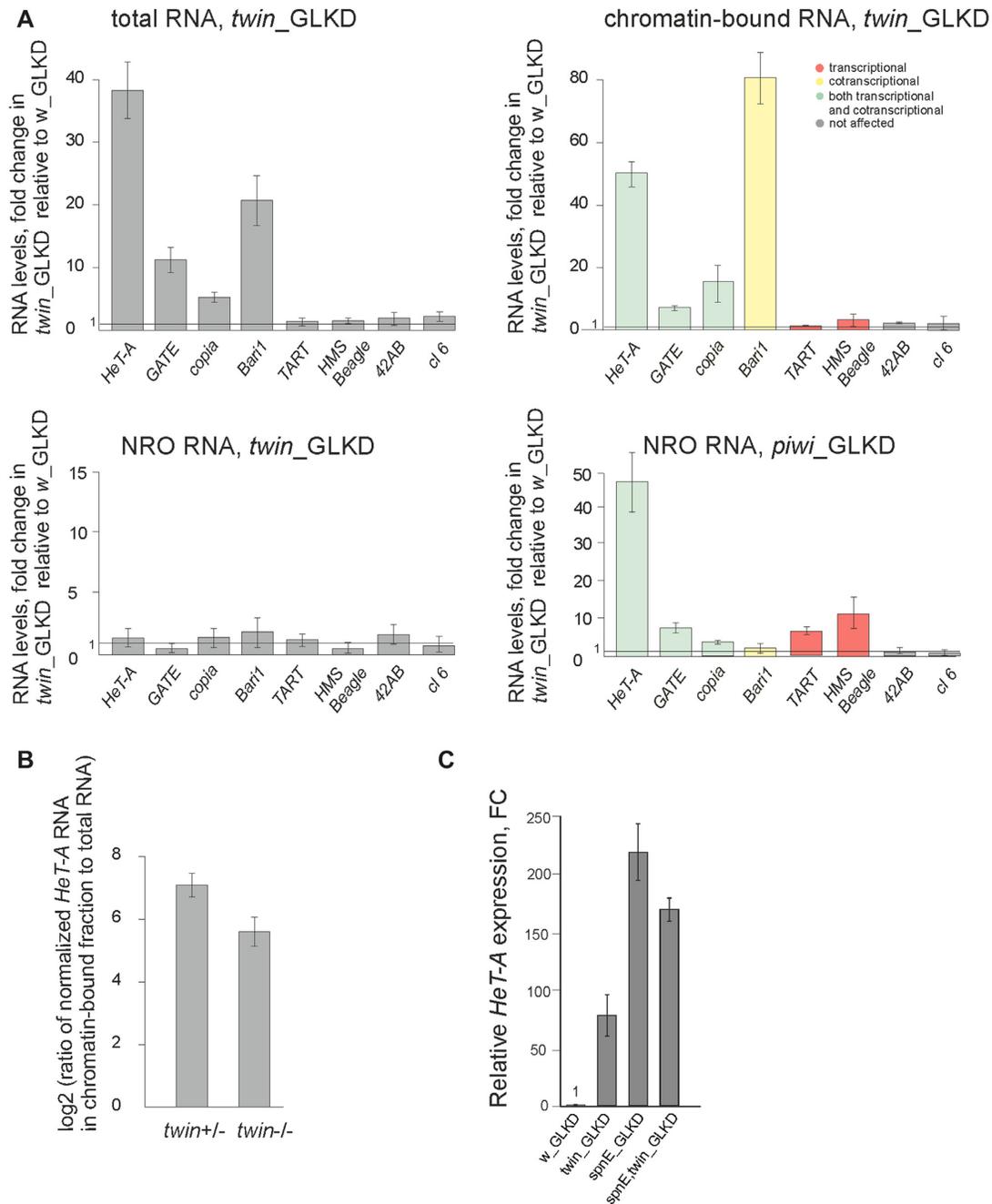
Figure 3. Ccr4 depletion causes the accumulation of TE transcripts in chromatin but does not affect their transcription state. (**A**) RT-qPCR analysis of expression of indicated TEs and piRNA clusters in total, NRO and chromatin-associated ovarian RNA fractions in *twin*_GLKD flies and in the NRO fraction of *piwi*_GLKD ovaries. The values were normalized to the TE copy number estimated by qPCR on the genomic DNA. The color of the bars indicates the type of TE regulation according to our data. (**B**) RT-qPCR analysis of *HeT-A* RNA, demonstrating its retention in chromatin. The *HeT-A* RNA level was normalized to *rp49*. The mean values (± standard deviation, SD) for two biological samples are shown. (**C**) Comparison of *HeT-A* transcript abundance in the ovaries of *twin*_GLKD, *spnE_GLKD* and *spnE, twin* double GLKD flies by RT-qPCR. The fold change in the *HeT-A* RNA level is shown. The mean values (±SD) for three biological samples are shown.

tion treatments (62). First, we performed immunostaining for Not1 and the telomere-specific protein HipHop (75) in wild-type ovaries. While overall Not1 staining in the nurse cell nuclei was faint, distinct Not1 foci were clearly detected. Moreover, most of the Not1 foci were grouped near telomeres (Figure 4A and B). Notably, in *piwi* and *spnE*_GLKD, the number of telomeric Not1 foci was strongly decreased (Figure 4A and B). Accordingly, telomeric Not1 foci were not detected in *piwi* and *spnE* mutants (Supplementary Figure S6). In *Not1*_GLKD ovaries, Not1 foci were not revealed, confirming their specificity (Supplementary Figure S6).

Ccr4 and Not1 form sparse but clearly distinguishable foci in the nurse cell nuclei (Figure 4C). We have revealed 4.2 ± 1.6 distinct Ccr4-Not foci per nucleus; 1.9 ± 0.9 of them colocalize with telomeres (HipHop staining) ($n = 14$). In *twin*_GLKD, Not1 foci were not detected, suggesting that Ccr4 is required for the assembly of telomeric Ccr4-Not foci (Figure 4A). The efficiency of the germline knockdowns was justified by western blotting (Supplementary Figure S5).

We observed that Not1 foci associate only with 12% of HipHop signals in the control ovaries. Ccr4-Not complexes are most likely locally accumulated only at telomeres enriched by tandem *HeT-A* arrays, which makes Ccr4-Not foci detectable by immunostaining. ChIP analysis of Ccr4-HA and Not1, even after dual cross-linking in the ovaries of a strain expressing Ccr4-HA, did not detect the association of these proteins with *HeT-A* chromatin (Supplementary Figure S7). Thus, Ccr4-Not can accumulate in close vicinity to telomeric chromatin in a piRNA-dependent manner, but this complex is not a chromatin component of telomeres. Notably, in the fission yeast *Schizosaccharomyces pombe*, the noncanonical poly(A) polymerase Cid14 is involved in the exosome-mediated degradation of heterochromatic RNAs and functions in close proximity to chromatin (76).

In fission yeast, the CCR4-NOT complex plays a role in heterochromatin formation at meiotic genes and subtelomeres (77). To test whether nuclear Ccr4-Not is involved in chromatin assembly in *Drosophila* ovaries, we examined how Ccr4 depletion affects the TE and piRNA cluster chromatin structure using ChIP. We did not detect any significant changes in the association of HP1, Rhino and H3K9me3 chromatin components with piRNA clusters and TEs, including *HeT-A, copia* and *Bari1* families, which showed a pronounced increase in chromatin-bound RNA levels in Ccr4 mutants (Figure 4D). This result is in accordance with the absence of transcriptional changes demonstrated by the NRO assay in *twin*_GLKD for these TEs (Figure 3A). ChIP was complemented with *HeT-A* DNA FISH combined with Rhi immunostaining. In contrast to piRNA pathway mutants, where *HeT-A*s lose HP1, Rhi and H3K9me3 (42,70,78), *HeT-A* signals overlap with Rhi in nurse cell nuclei upon *twin*_GLKD (Figure 4E) and in *twin* mutants (Supplementary Figure S8A). TAS DNA FISH signals also colocalize with Rhi in *twin* mutants (Supplementary Figure S8B). Thus, in contrast to yeast, the nuclear Ccr4-Not complex does not participate in heterochromatin assembly at its targets in the *Drosophila* ovaries.

Taken together, our data indicate that Ccr4 could act downstream of the piRNA-mediated TGS, promoting the degradation of TE-derived RNAs in the nucleus at the transcription sites.

Ccr4 depletion does not affect piRNA production

In *Caenorhabditis elegans*, Ccr4-Not components were identified among factors required for siRNA generation from their endogenous targets (79). To address the role of Ccr4 in small RNA biogenesis, we sequenced small RNAs from the ovaries of hypomorphic and catalytic Ccr4 mutants. By mapping small RNAs, we did not reveal differences in the abundance of piRNA cluster-derived or TE-derived piRNAs between heterozygous and transheterozygous mutants (Figure 5A and B; Supplementary Figure S9). A characteristic feature of the ping-pong piRNA amplification mechanism is the number of complementary piRNA pairs with a 10-nucleotide overlap between their 5′ ends (24,39). The ping-pong piRNA profiles of TEs expressed in the germline were also highly similar in *twin* hetero and transheterozygous mutants (Supplementary Figure S9). Thus, Ccr4 participates in the silencing of piRNA targets but acts downstream of piRNA production and amplification.

Dispersed transcriptionally active TE copies located outside of piRNA clusters become novel piRNA clusters that induce piRNA production from TE-flanking genomic regions (28). A hallmark of TE-associated piRNAs is that these piRNAs are produced from opposing genomic strands upstream and downstream of the TE insertion. TE insertion sites in the genome of *twin DG^{24102}/Df(3R)crb87-4* strain were predicted using genome sequencing data. A strong flanking piRNA signature was revealed for Ccr4-targeted TEs, and their levels were similar in control ovaries and *twin* mutants (Figure 5C). For example, Ccr4 depletion does not affect the flanking piRNA signature of the euchromatic *Bari* transposon but leads to the accumulation of its transcripts in the chromatin-bound RNA fraction (Figure 5D). Thus, Ccr4 predominantly targets standalone TEs that produce piRNA precursors but does not compete with the piRNA processing machinery for the emerging transcripts.

Ccr4-Not interacts with piRNA pathway components in the nucleus

To reveal the interactions between nuclear Ccr4-Not and the piRNA pathway components, we carried out co-immunopurification experiments using nuclear protein extracts. Cell fractionation of the ovaries followed by western blotting shows that the nuclear fraction is enriched by HP1 but not by cytoplasmic proteins (Supplementary Figure S10). Transgenic strains expressing HA-tagged Ccr4 and Piwi-GFP in the germline were used for the analysis. First, we revealed the presence of Ccr4-HA in complex with Piwi-GFP (Figure 6A). Piwi and Not1 were copurified with Ccr4-HA (Figure 6B), which confirms that Piwi associates with the Ccr4-Not complex. Cutoff (Cuff) is a protein involved in the 3′ end RNA processing of piRNA precursors in flies (31,34). Next, we addressed the question con-
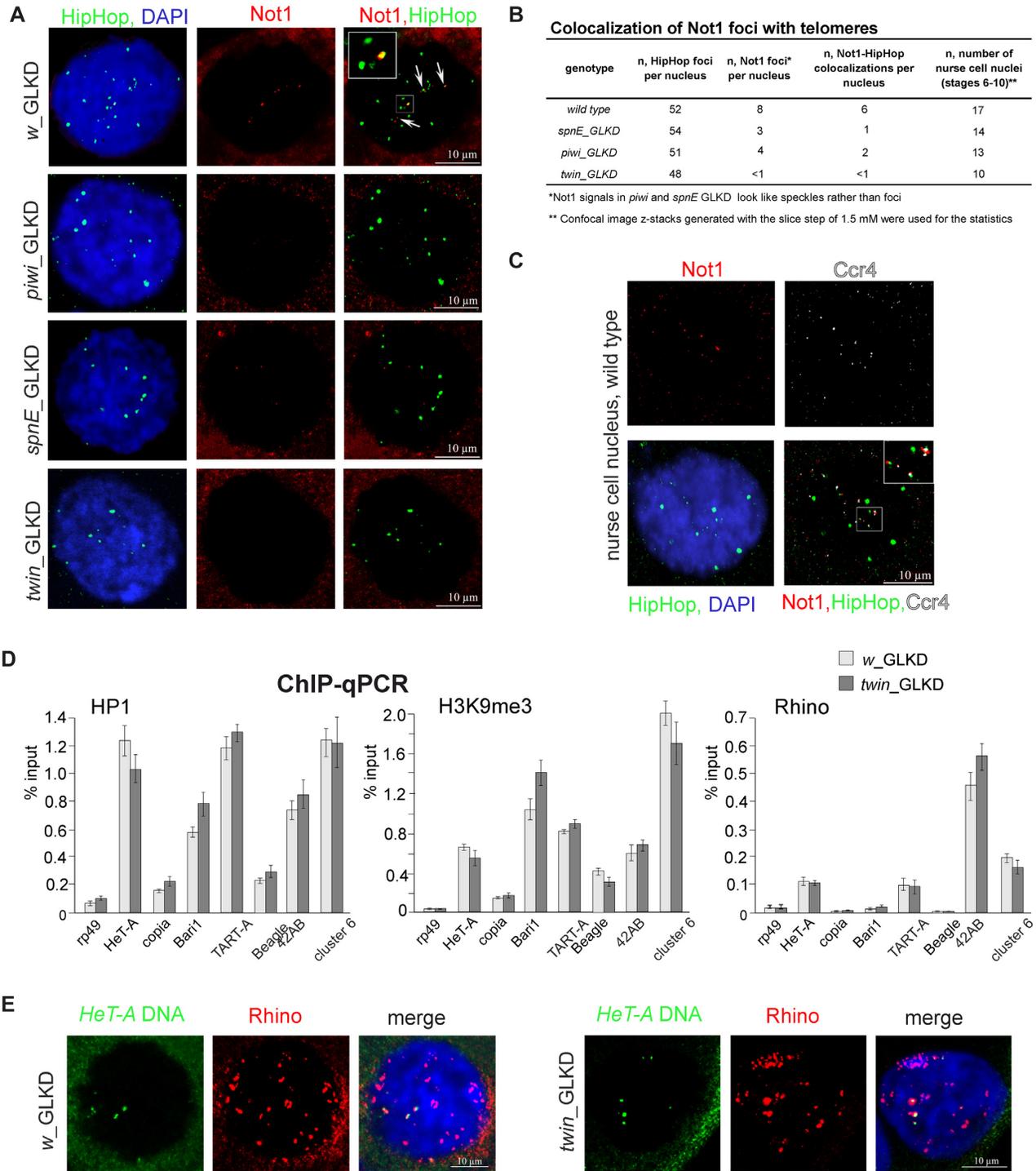
Figure 4. The Ccr4-Not complex is located near chromatin but does not affect the chromatin state of its targets. (**A**) Not1 (red) and HipHop (green) immunostaining was performed on the ovaries of *yw*, *piwi*_GLKD, *spnE*_GLKD and *twin*_GLKD flies. The nuclei of nurse cells from the VIII–X stages of oogenesis are shown. Most Not1 foci colocalize with telomeres (arrows) in wild-type ovaries. The boxed area is enlarged. (**B**) Table showing the colocalization statistics of Not1 foci and telomeres in the nurse cell nuclei of the indicated strains. (**C**) Not1 (red) and Ccr4 (gray) immunostaining signals colocalize at telomeres marked by HipHop (green) in the nurse cell nuclei of the control *yw* strain. The boxed area is enlarged. (**D**) ChIP-qPCR analysis of HP1, Rhino and H3K9me3 at TE and piRNA cluster sequences in the ovaries of *w*_GLKD and *twin*_GLKD. Euchromatic gene *rp49* is included in the analysis as a negative control. (**E**) DNA FISH with *HeT-A* probe (green) combined with Rhi staining (red) was performed on the ovaries of *w*_GLKD and *twin*_GLKD flies. DNA was stained with DAPI (blue). The nuclei of nurse cells from the VIII–X stages of oogenesis are shown.
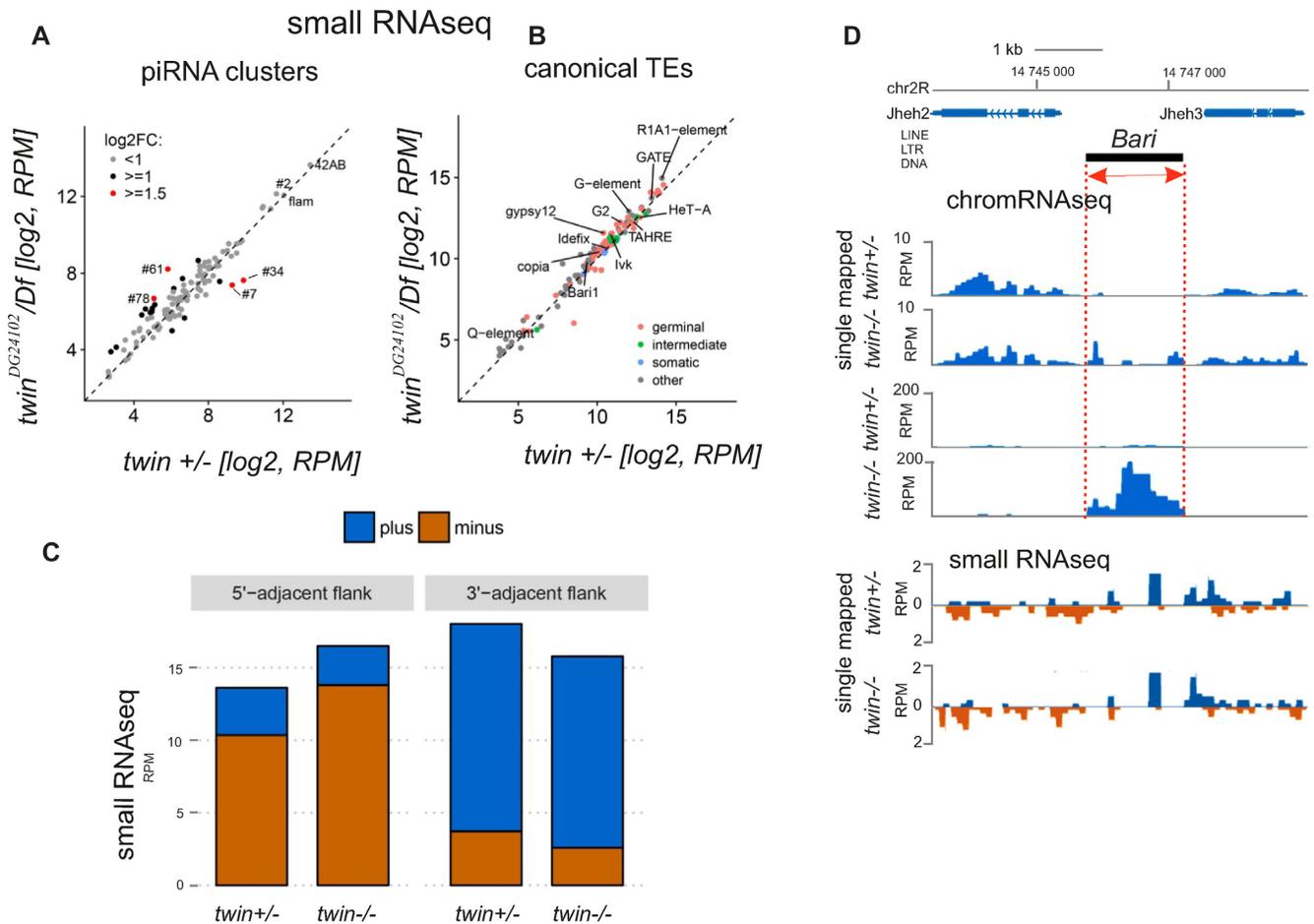
Figure 5. Ccr4 does not affect small RNA production. Scatter plots of log$_2$-transformed and RPM-normalized small RNA expression in the ovaries of *twin^{DG24102}/Df* mutants. Small RNAs mapped to piRNA clusters (**A**) and canonical TEs (**B**) are shown. The color of the dots indicates the type of TEs according to their transcription patterns in ovaries. (**C**) The abundance and strand-specificity of 5′ and 3′ flanking piRNAs produced by Ccr4 TE targets (from Supplementary Table S1). Ccr4 mutations (*twin^{DG24102}/Df*) do not affect the flanking piRNA signature of stand-alone TEs. (**D**) The effect of Ccr4 mutation on the level of chromatin-associated and small RNAs corresponding to the euchromatic site of the *Bari1* transposon insertion. Dotted lines indicate the borders of TE.

cerning the interaction between nuclear Ccr4-Not and Cuff. Co-IP experiments performed with Ccr4-HA- and Cuff-GFP-expressing transgenic strains revealed an association between these proteins. However, we did not detect the association of Ccr4 with the chromatin protein Rhi (Figure 6C and Supplementary Figure S10). Notably, the ratio between protein levels in input and co-IP samples indicates that only a small fraction of Piwi and Cuff interacts with Ccr4-Not. Thoc5, a component of the mRNA nuclear export complex THO/TREX, was copurified with the Ccr4-Not complex (Figure 6B and D), indicating a link between *Drosophila* Ccr4-Not and nuclear export machinery, similar to that observed in yeast (15).

Upon *piwi*_GLKD, Ccr4 is revealed in the Not1 complex, indicating that this interaction is Piwi-independent. Thoc5 is also copurified with Not1 upon *piwi* depletion, though less efficiently than in wild-type ovaries (Figure 6D).

To confirm the results of coimmunoprecipitation experiments, we have performed coimmunostaining of wild type ovaries and statistical analysis of 3D confocal images of the nurse cell nuclei. We have revealed 2.4 ± 1.8 Ccr4-Piwi

foci colocalizing with telomeres (HipHop staining) per nucleus (*n* = 9). Thoc5 and Cuff-GFP staining is observed at many telomeres (Supplementary Figure S11); on average, 1.4 ± 0.7 colocalization sites of Not1 with Thoc5 and 2.1 ± 0.9 colocalization sites of Not1 with Cuff-GFP per nucleus were detected at telomeres (*n* = 10, Figure 6E). Interestingly, the accumulation of these proteins near telomeres leads to the formation of the structures that can be referred to as telomeric bodies.

These data suggest that the nuclear Ccr4-Not complex cooperates with piRNA pathway components for the degradation of the telomeric transcripts and probably the other TE transcripts recognized by piRNAs in the germline (Figure 6F).

DISCUSSION

Our data revealed a new layer of anti-transposon control in the germline acting in the nucleus at the sites of transcription. This mechanism is mediated by the nuclear deadenylase Ccr4-Not complex and involves the post-
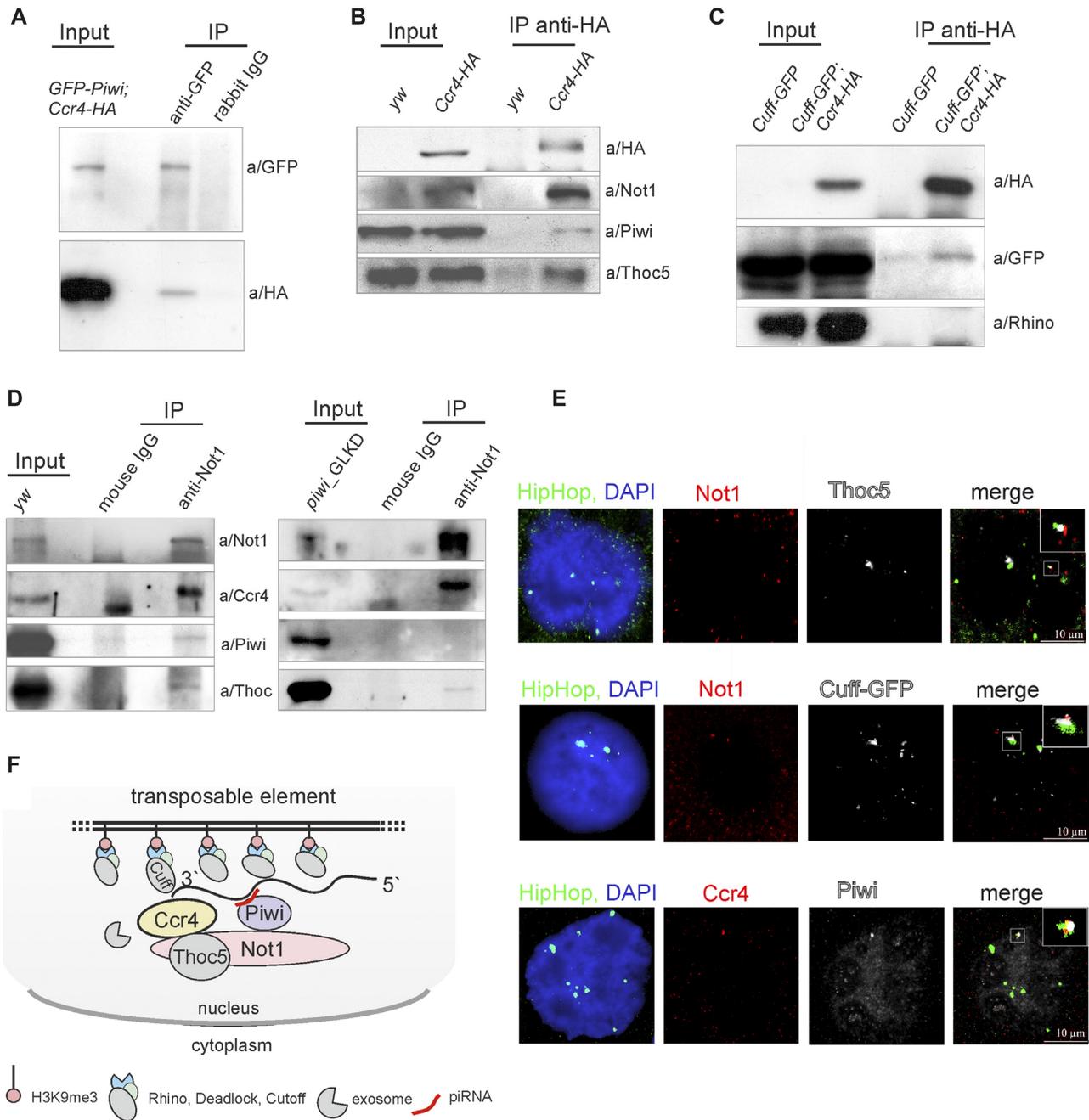
Figure 6. The Ccr4-Not complex is associated with piRNA pathway components. (**A**–**D**) Co-IP experiments were performed on ovarian nuclear extracts. The samples were separated by SDS-PAGE and analyzed by western blotting using the antibodies indicated on the right. The starting lysate (input) and immunoprecipitated probes (IP) are indicated; the antibodies used for co-IP are indicated above the IP lanes. (A) Co-IP was performed on the ovaries from the strain expressing Ccr4-HA and Piwi-GFP using anti-GFP antibodies. (B) Co-IP was performed on the ovaries of the *yw* and Ccr4-HA-expressing strains using anti-HA beads. (C) Co-IP was performed on the ovaries from the strain expressing Ccr4-HA and Cuff-GFP using anti-HA beads. Control co-IP was performed on the ovaries from the strain expressing only Cuff-GFP using anti-HA beads. (D) Co-IP was performed on the ovaries of the *yw* and *piwi*_GLKD strains using an anti-Not1 antibody. (**E**) Coimmunostaining demonstrating the colocalization of Ccr4-Not components (red) and Thoc5/Cutoff/Piwi (gray) at telomeres marked by HipHop (green) in the nurse cell nuclei of the control *yw* strain. The boxed areas are enlarged. (**F**) A model for the role of the Ccr4-Not complex in the degradation of transcripts recognized by piRNAs.

transcriptional degradation of active TE transcripts at transcription sites. The main question is how the RNA surveillance system can distinguish its substrates from 'right' RNA molecules. Our data indicate that Ccr4-Not may cooperate with the nuclear piRNA pathway to select its targets in the germline. We found that nuclear Ccr4-Not interacts with Piwi in *Drosophila* ovaries, which likely defines Ccr4-Not targets and leads to the cotranscriptional recognition and degradation of TE transcripts in the nucleus. The main targets of nuclear Ccr4-mediated silencing are full-length active TEs related to different families. We speculate that nuclear Ccr4 is directed by piRNA–Piwi complexes to the transcripts of TEs that are ineffectively silenced at the transcriptional level and therefore produce excessive transcripts. The cytoplasmic Piwi subfamily protein, Aub, recruits the Ccr4 complex to distinct mRNAs, leading to their translational repression (13,14). These data suggest that the Argonaute protein-mediated recruitment of Ccr4 to cognate RNAs is likely a conserved mechanism of the posttranscriptional control of gene expression. However, not all full-length TE copies are Ccr4-Not targets, suggesting a role for other factors in the selectivity of nuclear Ccr4-Not to particular TEs. Structural peculiarities, partner proteins or genomic context likely define emerging transposon RNAs for degradation in the nucleus. Interestingly, TAS regions consisting of complex satellites (80) are also overexpressed in Ccr4 mutants, suggesting that these repeats are actively transcribed, although the nature of their promoters is unclear.

The main telomeric retrotransposon, *HeT-A,* is the most sensitive target of the nuclear Ccr4-Not complex, indicating that RNA surveillance and telomere regulation are closely linked. Actually, *HeT-A* transcripts combine the features of both telomeric RNA (TERRA) and the telomerase RNA template, while in most species, these transcripts are separately regulated. RNA quality control mechanisms have been implicated in the biogenesis of both TERRA and telomerase RNA components. Indeed, nonsense-mediated mRNA decay (NMD) components hold a small fraction of deadenylated TERRA near telomeres, where telomeric RNAs seem to play a structural role (72). In *Saccharomyces cerevisiae,* the exonuclease Rat1p associates with telomeres and degrades TERRA molecules to maintain low TERRA levels (81). Unconventional human Ccr4 and Caf1 deadenylases are concentrated in nuclear Cajal bodies enriched in telomerase RNA, suggesting a role for the nuclear deadenylase complex in telomerase RNA biogenesis (82). We show here that the *Drosophila* Ccr4-Not complex participates in the cotranscriptional degradation of the nascent *HeT-A* transcripts near telomeres but plays a minor role in their retention at telomeres, suggesting that this process is regulated via a yet unknown mechanism. Previously, we reported that Ccr4 depletion led to an increase in *HeT-A* poly(A) length in total and nuclear ovarian RNA fractions (21). One may suggest that *HeT-A* RNAs that are retained at chromatin lack the poly(A) tail while polyadenylated *HeT-A* transcripts are promptly released from chromatin to the nucleoplasm and then exported to the cytoplasm. However, this essential point requires further investigation. In *S. pombe,* the HP1 homolog, HP1^{Swi6}, mediates the sequestration of heterochromatic RNAs at the sites of transcription, followed

by their destruction by nuclear RNA degradation enzymes (76). We suggest that one of two *Drosophila* HP1 homologs acting at telomeres in the germline, Rhi or HP1a, may serve to maintain the proper level of telomeric retroelement *HeT-A* RNA near chromatin. Intriguingly, Ccr4-Not complexes accumulate in foci near telomeres in a Piwi-dependent manner and colocalize with the piRNA pathway and RNA nuclear export components, forming telomeric bodies. The spatial proximity of different proteins acting at telomeres likely facilitates the assembly of these particles. It is tempting to speculate that the components of different nuclear RNA surveillance pathways cooperate to ensure the proper nuclear biogenesis of telomeric transcripts in the germline.

The distribution of Ccr4-Not in the nucleus suggests that these complexes act by scanning nascent transcripts. Indeed, only a few Ccr4-Not foci were revealed near telomeres, likely because of the local accumulation of deadenylase complexes at long *HeT-A* arrays. A scanning mechanism was recently reported for Piwi recruitment to its nuclear targets (83). It is likely that the Piwi–piRNA complex recruits the Ccr4-Not deadenylase complex to piRNA complementary transcripts, ensuring RNA quality control specific for the germline.

In fission yeast, the CCR4-NOT-mediated degradation of nascent transcripts is required for heterochromatin assembly at subtelomeres, developmentally regulated genes and retrotransposons (77,84,85). Moreover, in *C. elegans*, Ccr4 is required for siRNA generation from their endogenous targets (79). However, the depletion of *Drosophila* Ccr4 does not affect piRNA production and chromatin changes at its targets in the germline, suggesting that the role of the nuclear deadenylase complex in *Drosophila* is restricted by the degradation of TE transcripts at transcription sites. In fission yeast, an interaction between CCR4–NOT, the exosome and its nuclear cofactor TRAMP ensures RNA degradation in the nucleus (16). According to the current model, the yeast CCR4-NOT complex could be required as a structural component of nuclear RNA surveillance, creating an opportunity for exosome to trigger the 3′–5′ degradation of the nascent RNA (86). However, the germline knockdowns of Rrp6 and Dis3, the fly homologs of the yeast 3′–5′ exonucleases RRP6 and RRP44, respectively (87), result in severe ovary degeneration, making expression analysis impracticable. The role of nuclear exosome in the cotranscriptional Ccr4-Not-mediated degradation of TE transcripts in the *Drosophila* germline remains to be investigated.

The chromatin complex comprising Rhi, Deadlock and Cuff mediates the transcription of piRNA precursors from dual-strand piRNA clusters (31,34). Cuff guides the loading of TREX onto piRNA precursors, followed by their export from the nucleus into the cytoplasmic piRNA processing machinery (35,36). We revealed the interaction between Ccr4 and Cuff, most likely because both proteins are involved in 3′ end RNA processing. Not1 likely serves as a structural platform for the binding of components related to different regulatory pathways, providing their functional interplay (Figure 6, a model). The association between Ccr4 and Cuff, a hallmark of piRNA clusters (31), suggests that Ccr4 TE targets are related to dual-strand piRNA clusters, but heterochromatic piRNA clusters are not af-

fected by the Ccr4-Not complex. This finding is not surprising considering the existence of different types of Rhi-dependent piRNA clusters. Pericentromeric piRNA clusters comprising TE fragments use noncanonical promoter-independent transcription (31,33). Telomeric piRNA clusters (70) and individual copies of recently transposed TEs (28) are related to actively transcribed piRNA clusters possessing canonical promoters. Our data show that Ccr4 regulates the expression of telomeric, subtelomeric and TE-associated piRNA clusters. The flanking piRNA signature, a characteristic of TE-associated piRNA clusters, was revealed for Ccr4 TE targets. This fact suggests that TE transcripts emerging from the same locus are guided to both piRNA processing and Ccr4-mediated degradation. However, Ccr4 depletion does not affect piRNA production, suggesting that the Ccr4-Not-mediated degradation of TE transcripts does not interfere with the generation and export of piRNA precursors at the same locus. In fission yeast, heterochromatic and transposon transcripts are more actively processed by RNAi machinery in the absence of nuclear exosome (88,89). In contrast, TE transcripts accumulated in Ccr4-depleted *Drosophila* ovaries avoid piRNA-mediated degradation. Under normal conditions, TE transcripts may be prevented from recruiting export factors by Ccr4-Not. In the absence of Ccr4-Not, these transcripts being polyadenylated are recognized as export-competent mRNAs, followed by their delivery to translational machinery, bypassing piRNA production compartments. In parallel, alternative 3′ end processing with the participation of Cuff defines a fraction of TE RNAs for piRNA processing (34).

piRNAs have been implicated in the transcriptional silencing and *de novo* piRNA production at active TEs. Our data suggest that the piRNA–Piwi complex can also recruit nuclear Ccr4-Not to degrade abundant TE transcripts at chromatin. Altogether, these mechanisms ensure a powerful multilevel defense against transpositionally competent transposons.

DATA AVAILABILITY

Two replicates of chromatin-bound RNA-seq data for *twin ^{DG24102}/Df(3R)crb87-4* and ovarian small RNA-seq data for *twin^{S1}/twin^{S3}* and *twin ^{DG24102}/Df(3R)crb87-4* were deposited at Gene Expression Omnibus (GEO), accession number GSE120412. Deep sequencing data of genomic DNA of *twin ^{DG24102}/Df(3R)crb87-4* strain were deposited in the NCBI SRA database SRR7949510.

SUPPLEMENTARY DATA

Supplementary Data are available at NAR Online.

REFERENCES

1. Goldstrohm,A.C. and Wickens,M. (2008) Multifunctional deadenylase complexes diversify mRNA control. *Nat. Rev. Mol. Cell Biol.*, **9**, 337–344.
2. Collart,M.A. and Panasenko,O.O. (2012) The Ccr4–not complex. *Gene*, **492**, 42–53.
3. Collart,M.A. (2016) The Ccr4-Not complex is a key regulator of eukaryotic gene expression. *Wiley Interdiscip. Rev. RNA*, **7**, 438–454.
4. Chicoine,J., Benoit,P., Gamberi,C., Paliouras,M., Simonelig,M. and Lasko,P. (2007) Bicaudal-C recruits CCR4-NOT deadenylase to target mRNAs and regulates oogenesis, cytoskeletal organization, and its own expression. *Dev. Cell*, **13**, 691–704.
5. Morris,J.Z., Hong,A., Lilly,M.A. and Lehmann,R. (2005) twin, a CCR4 homolog, regulates cyclin poly(A) tail length to permit Drosophila oogenesis. *Development*, **132**, 1165–1174.
6. Temme,C., Zhang,L., Kremmer,E., Ihling,C., Chartier,A., Sinz,A., Simonelig,M. and Wahle,E. (2010) Subunits of the Drosophila CCR4-NOT complex and their roles in mRNA deadenylation. *RNA*, **16**, 1356–1370.
7. Zaessinger,S., Busseau,I. and Simonelig,M. (2006) Oskar allows nanos mRNA translation in Drosophila embryos by preventing its deadenylation by Smaug/CCR4. *Development*, **133**, 4573–4583.
8. Temme,C., Zaessinger,S., Meyer,S., Simonelig,M. and Wahle,E. (2004) A complex containing the CCR4 and CAF1 proteins is involved in mRNA deadenylation in Drosophila. *EMBO J.*, **23**, 2862–2871.
9. Lasko,P. (2012) mRNA localization and translational control in Drosophila oogenesis. *Cold Spring Harb. Perspect. Biol.*, **4**, a012294.
10. Zekri,L., Huntzinger,E., Heimstadt,S. and Izaurralde,E. (2009) The silencing domain of GW182 interacts with PABPC1 to promote translational repression and degradation of microRNA targets and is required for target release. *Mol. Cell Biol.*, **29**, 6220–6231.
11. Fabian,M.R., Mathonnet,G., Sundermeier,T., Mathys,H., Zipprich,J.T., Svitkin,Y.V., Rivas,F., Jinek,M., Wohlschlegel,J., Doudna,J.A. *et al.* (2009) Mammalian miRNA RISC recruits CAF1 and PABP to affect PABP-dependent deadenylation. *Mol. Cell*, **35**, 868–880.
12. Piao,X., Zhang,X., Wu,L. and Belasco,J.G. (2010) CCR4-NOT deadenylates mRNA associated with RNA-induced silencing complexes in human cells. *Mol. Cell Biol.*, **30**, 1486–1494.
13. Rouget,C., Papin,C., Boureux,A., Meunier,A.C., Franco,B., Robine,N., Lai,E.C., Pelisson,A. and Simonelig,M. (2010) Maternal mRNA deadenylation and decay by the piRNA pathway in the early Drosophila embryo. *Nature*, **467**, 1128–1132.
14. Rojas-Rios,P., Chartier,A., Pierson,S. and Simonelig,M. (2017) Aubergine and piRNAs promote germline stem cell self-renewal by repressing the proto-oncogene Cbl. *EMBO J.*, **36**, 3194–3211.
15. Kerr,S.C., Azzouz,N., Fuchs,S.M., Collart,M.A., Strahl,B.D., Corbett,A.H. and Laribee,R.N. (2011) The Ccr4-Not complex interacts with the mRNA export machinery. *PLoS One*, **6**, e18302.
16. Azzouz,N., Panasenko,O.O., Colau,G. and Collart,M.A. (2009) The CCR4-NOT complex physically and functionally interacts with TRAMP and the nuclear exosome. *PLoS One*, **4**, e6760.
17. Eberle,A.B. and Visa,N. (2014) Quality control of mRNP biogenesis: networking at the transcription site. *Semin. Cell Dev. Biol.*, **32**, 37–46.
18. Rougemaille,M., Gudipati,R.K., Olesen,J.R., Thomsen,R., Seraphin,B., Libri,D. and Jensen,T.H. (2007) Dissecting mechanisms

of nuclear mRNA surveillance in THO/sub2 complex mutants. *EMBO J.*, **26**, 2317–2326.

19. Luna,R., Rondon,A.G. and Aguilera,A. (2012) New clues to understand the role of THO and other functionally related factors in mRNP biogenesis. *Biochim. Biophys. Acta*, **1819**, 514–520.

20. de Almeida,S.F., Garcia-Sacristan,A., Custodio,N. and Carmo-Fonseca,M. (2010) A link between nuclear RNA surveillance, the human exosome and RNA polymerase II transcriptional termination. *Nucleic Acids Res.*, **38**, 8015–8026.

21. Morgunova,V., Akulenko,N., Radion,E., Olovnikov,I., Abramov,Y., Olenina,L.V., Shpiz,S., Kopytova,D.V., Georgieva,S.G. and Kalmykova,A. (2015) Telomeric repeat silencing in germ cells is essential for early development in Drosophila. *Nucleic Acids Res.*, **43**, 8762–8773.

22. Lim,A.K., Tao,L. and Kai,T. (2009) piRNAs mediate posttranscriptional retroelement silencing and localization to pi-bodies in the Drosophila germline. *J. Cell Biol.*, **186**, 333–342.

23. Savitsky,M., Kwon,D., Georgiev,P., Kalmykova,A. and Gvozdev,V. (2006) Telomere elongation is under the control of the RNAi-based mechanism in the Drosophila germline. *Genes Dev.*, **20**, 345–354.

24. Brennecke,J., Aravin,A.A., Stark,A., Dus,M., Kellis,M., Sachidanandam,R. and Hannon,G.J. (2007) Discrete small RNA-generating loci as master regulators of transposon activity in Drosophila. *Cell*, **128**, 1089–1103.

25. Iwasaki,Y.W., Siomi,M.C. and Siomi,H. (2015) PIWI-Interacting RNA: Its biogenesis and functions. *Annu. Rev. Biochem.*, **84**, 405–433.

26. Ozata,D.M., Gainetdinov,I., Zoch,A., O'Carroll,D. and Zamore,P.D. (2019) PIWI-interacting RNAs: small RNAs with big functions. *Nat. Rev. Genet.*, **20**, 89–108.

27. Aravin,A.A., Sachidanandam,R., Bourc'his,D., Schaefer,C., Pezic,D., Toth,K.F., Bestor,T. and Hannon,G.J. (2008) A piRNA pathway primed by individual transposons is linked to de novo DNA methylation in mice. *Mol. Cell*, **31**, 785–799.

28. Shpiz,S., Ryazansky,S., Olovnikov,I., Abramov,Y. and Kalmykova,A. (2014) Euchromatic transposon insertions trigger production of novel Pi- and endo-siRNAs at the target sites in the drosophila germline. *PLos Genet.*, **10**, e1004138.

29. Song,J., Liu,J., Schnakenberg,S.L., Ha,H., Xing,J. and Chen,K.C. (2014) Variation in piRNA and transposable element content in strains of Drosophila melanogaster. *Genome Biol. Evol.*, **6**, 2786–2798.

30. Klattenhoff,C., Xi,H., Li,C., Lee,S., Xu,J., Khurana,J.S., Zhang,F., Schultz,N., Koppetsch,B.S., Nowosielska,A. *et al.* (2009) The Drosophila HP1 homolog Rhino is required for transposon silencing and piRNA production by dual-strand clusters. *Cell*, **138**, 1137–1149.

31. Mohn,F., Sienski,G., Handler,D. and Brennecke,J. (2014) The rhino-deadlock-cutoff complex licenses noncanonical transcription of dual-strand piRNA clusters in Drosophila. *Cell*, **157**, 1364–1379.

32. Rangan,P., Malone,C.D., Navarro,C., Newbold,S.P., Hayes,P.S., Sachidanandam,R., Hannon,G.J. and Lehmann,R. (2011) piRNA production requires heterochromatin formation in Drosophila. *Curr. Biol.*, **21**, 1373–1379.

33. Andersen,P.R., Tirian,L., Vunjak,M. and Brennecke,J. (2017) A heterochromatin-dependent transcription machinery drives piRNA expression. *Nature*, **549**, 54–59.

34. Chen,Y.C., Stuwe,E., Luo,Y., Ninova,M., Le Thomas,A., Rozhavskaya,E., Li,S., Vempati,S., Laver,J.D., Patel,D.J. *et al.* (2016) Cutoff suppresses RNA polymerase II termination to ensure expression of piRNA precursors. *Mol. Cell*, **63**, 97–109.

35. Hur,J.K., Luo,Y., Moon,S., Ninova,M., Marinov,G.K., Chung,Y.D. and Aravin,A.A. (2016) Splicing-independent loading of TREX on nascent RNA is required for efficient expression of dual-strand piRNA clusters in Drosophila. *Genes Dev.*, **30**, 840–855.

36. Zhang,F., Wang,J., Xu,J., Zhang,Z., Koppetsch,B.S., Schultz,N., Vreven,T., Meignin,C., Davis,I., Zamore,P.D. *et al.* (2012) UAP56 couples piRNA clusters to the perinuclear transposon silencing machinery. *Cell*, **151**, 871–884.

37. Zhang,G., Tu,S., Yu,T., Zhang,X.O., Parhad,S.S., Weng,Z. and Theurkauf,W.E. (2018) Co-dependent assembly of Drosophila piRNA precursor Complexes and piRNA cluster heterochromatin. *Cell Rep.*, **24**, 3413–3422.

38. Pane,A., Jiang,P., Zhao,D.Y., Singh,M. and Schupbach,T. (2011) The Cutoff protein regulates piRNA cluster expression and piRNA production in the Drosophila germline. *EMBO J.*, **30**, 4601–4615.

39. Gunawardane,L.S., Saito,K., Nishida,K.M., Miyoshi,K., Kawamura,Y., Nagami,T., Siomi,H. and Siomi,M.C. (2007) A slicer-mediated mechanism for repeat-associated siRNA 5′ end formation in Drosophila. *Science*, **315**, 1587–1590.

40. Han,B.W., Wang,W., Li,C., Weng,Z. and Zamore,P.D. (2015) Noncoding RNA. piRNA-guided transposon cleavage initiates Zucchini-dependent, phased piRNA production. *Science*, **348**, 817–821.

41. Mohn,F., Handler,D. and Brennecke,J. (2015) Noncoding RNA. piRNA-guided slicing specifies transcripts for Zucchini-dependent, phased piRNA biogenesis. *Science*, **348**, 812–817.

42. Rozhkov,N.V., Hammell,M. and Hannon,G.J. (2013) Multiple roles for Piwi in silencing Drosophila transposons. *Genes Dev.*, **27**, 400–412.

43. Sienski,G., Donertas,D. and Brennecke,J. (2012) Transcriptional silencing of transposons by piwi and maelstrom and its impact on chromatin state and gene expression. *Cell*, **151**, 964–980.

44. Kelleher,E.S. and Barbash,D.A. (2013) Analysis of piRNA-mediated silencing of active TEs in Drosophila melanogaster suggests limits on the evolution of host genome defense. *Mol. Biol. Evol.*, **30**, 1816–1829.

45. Buhler,M. (2009) RNA turnover and chromatin-dependent gene silencing. *Chromosoma*, **118**, 141–151.

46. Buhler,M. and Moazed,D. (2007) Transcription and RNAi in heterochromatic gene silencing. *Nat. Struct. Mol. Biol.*, **14**, 1041–1048.

47. Houseley,J., Kotovic,K., El Hage,A. and Tollervey,D. (2007) Trf4 targets ncRNAs from telomeric and rDNA spacer regions and functions in rDNA copy number control. *EMBO J.*, **26**, 4996–5006.

48. Buhler,M., Spies,N., Bartel,D.P. and Moazed,D. (2008) TRAMP-mediated RNA surveillance prevents spurious entry of RNAs into the Schizosaccharomyces pombe siRNA pathway. *Nat. Struct. Mol. Biol.*, **15**, 1015–1023.

49. Le Thomas,A., Rogers,A.K., Webster,A., Marinov,G.K., Liao,S.E., Perkins,E.M., Hur,J.K., Aravin,A.A. and Toth,K.F. (2013) Piwi induces piRNA-guided transcriptional silencing and establishment of a repressive chromatin state. *Genes Dev.*, **27**, 390–399.

50. Semotok,J.L., Cooperstock,R.L., Pinder,B.D., Vari,H.K., Lipshitz,H.D. and Smibert,C.A. (2005) Smaug recruits the CCR4/POP2/NOT deadenylase complex to trigger maternal transcript localization in the early Drosophila embryo. *Curr. Biol.*, **15**, 284–294.

51. Klenov,M.S., Sokolova,O.A., Yakushev,E.Y., Stolyarenko,A.D., Mikhaleva,E.A., Lavrov,S.A. and Gvozdev,V.A. (2011) Separation of stem cell maintenance and transposon silencing functions of Piwi protein. *Proc. Natl. Acad. Sci. U.S.A.*, **108**, 18760–18765.

52. Shpiz,S., Olovnikov,I., Sergeeva,A., Lavrov,S., Abramov,Y., Savitsky,M. and Kalmykova,A. (2011) Mechanism of the piRNA-mediated silencing of Drosophila telomeric retrotransposons. *Nucleic Acids Res.*, **39**, 8703–8711.

53. Kogan,G.L., Tulin,A.V., Aravin,A.A., Abramov,Y.A., Kalmykova,A.I., Maisonhaute,C. and Gvozdev,V.A. (2003) The GATE retrotransposon in Drosophila melanogaster: mobility in heterochromatin and aspects of its expression in germline tissues. *Mol. Genet. Genomics*, **269**, 234–242.

54. Picelli,S., Bjorklund,A.K., Reinius,B., Sagasser,S., Winberg,G. and Sandberg,R. (2014) Tn5 transposase and tagmentation procedures for massively scaled sequencing projects. *Genome Res.*, **24**, 2033–2040.

55. Langmead,B. and Salzberg,S.L. (2012) Fast gapped-read alignment with Bowtie 2. *Nat. Methods*, **9**, 357–359.

56. Olovnikov,I., Ryazansky,S., Shpiz,S., Lavrov,S., Abramov,Y., Vaury,C., Jensen,S. and Kalmykova,A. (2013) De novo piRNA cluster formation in the Drosophila germ line triggered by transgenes containing a transcribed transposon fragment. *Nucleic Acids Res.*, **41**, 5757–5768.

57. Akulenko,N., Ryazansky,S., Morgunova,V., Komarov,P.A., Olovnikov,I., Vaury,C., Jensen,S. and Kalmykova,A. (2018) Transcriptional and chromatin changes accompanying de novo formation of transgenic piRNA clusters. *RNA*, **24**, 574–584.

58. Radion,E., Ryazansky,S., Akulenko,N., Rozovsky,Y., Kwon,D., Morgunova,V., Olovnikov,I. and Kalmykova,A. (2017) Telomeric retrotransposon HeT-A contains a bidirectional promoter that initiates divergent transcription of piRNA precursors in Drosophila germline. *J. Mol. Biol.*, **429**, 3280–3289.

59. Zeng,P.Y., Vakoc,C.R., Chen,Z.C., Blobel,G.A. and Berger,S.L. (2006) In vivo dual cross-linking for identification of indirect DNA-associated proteins by chromatin immunoprecipitation. *Biotechniques*, **41**, 694.

60. Lavrov,S., Dejardin,J. and Cavalli,G. (2004) Combined immunostaining and FISH analysis of polytene chromosomes. *Methods Mol. Biol.*, **247**, 289–303.

61. Danilevskaya,O.N., Traverse,K.L., Hogan,N.C., DeBaryshe,P.G. and Pardue,M.L. (1999) The two Drosophila telomeric transposable elements have very different patterns of transcription. *Mol. Cell Biol.*, **19**, 873–881.

62. Kordyukova,M., Morgunova,V., Olovnikov,I., Komarov,P.A., Mironova,A., Olenkina,O.M. and Kalmykova,A. (2018) Subcellular localization and Egl-mediated transport of telomeric retrotransposon HeT-A ribonucleoprotein particles in the Drosophila germline and early embryogenesis. *PLoS One*, **13**, e0201787.

63. Kopytova,D.V., Orlova,A.V., Krasnov,A.N., Gurskiy,D.Y., Nikolenko,J.V., Nabirochkina,E.N., Shidlovskii,Y.V. and Georgieva,S.G. (2010) Multifunctional factor ENY2 is associated with the THO complex and promotes its recruitment onto nascent mRNA. *Genes Dev.*, **24**, 86–96.

64. Joly,W., Chartier,A., Rojas-Rios,P., Busseau,I. and Simonelig,M. (2013) The CCR4 deadenylase acts with Nanos and Pumilio in the fine-tuning of Mei-P26 expression to promote germline stem cell self-renewal. *Stem Cell Rep.*, **1**, 411–424.

65. Cenci,G., Siriaco,G., Raffa,G.D., Kellum,R. and Gatti,M. (2003) The Drosophila HOAP protein is required for telomere capping. *Nat. Cell Biol.*, **5**, 82–84.

66. Shpiz,S. and Kalmykova,A. (2014) Analyses of piRNA-mediated transcriptional transposon silencing in Drosophila: nuclear run-on assay on ovaries. *Methods Mol. Biol.*, **1093**, 149–159.

67. Kaminker,J.S., Bergman,C.M., Kronmiller,B., Carlson,J., Svirskas,R., Patel,S., Frise,E., Wheeler,D.A., Lewis,S.E., Rubin,G.M. *et al.* (2002) The transposable elements of the Drosophila melanogaster euchromatin: a genomics perspective. *Genome Biol.*, **3**, RESEARCH0084.

68. Danilevskaya,O.N., Arkhipova,I.R., Traverse,K.L. and Pardue,M.L. (1997) Promoting in tandem: the promoter for telomere transposon HeT-A and implications for the evolution of retroviral LTRs. *Cell*, **88**, 647–655.

69. Shpiz,S., Kwon,D., Uneva,A., Kim,M., Klenov,M., Rozovsky,Y., Georgiev,P., Savitsky,M. and Kalmykova,A. (2007) Characterization of Drosophila telomeric retroelement TAHRE: transcription, transpositions, and RNAi-based regulation of expression. *Mol. Biol. Evol.*, **24**, 2535–2545.

70. Radion,E., Morgunova,V., Ryazansky,S., Akulenko,N., Lavrov,S., Abramov,Y., Komarov,P.A., Glukhov,S.I., Olovnikov,I. and Kalmykova,A. (2018) Key role of piRNAs in telomeric chromatin maintenance and telomere nuclear positioning in Drosophila germline. *Epigenet. Chromatin*, **11**, 40.

71. Lis,J. (1998) Promoter-associated pausing in promoter architecture and postinitiation transcriptional regulation. *Cold Spring Harb. Symp. Quant. Biol.*, **63**, 347–356.

72. Azzalin,C.M., Reichenbach,P., Khoriauli,L., Giulotto,E. and Lingner,J. (2007) Telomeric repeat containing RNA and RNA surveillance factors at mammalian chromosome ends. *Science*, **318**, 798–801.

73. Malone,C.D., Brennecke,J., Dus,M., Stark,A., McCombie,W.R., Sachidanandam,R. and Hannon,G.J. (2009) Specialized piRNA pathways act in germline and somatic tissues of the Drosophila ovary. *Cell*, **137**, 522–535.

74. Vagin,V.V., Klenov,M.S., Kalmykova,A.I., Stolyarenko,A.D., Kotelnikov,R.N. and Gvozdev,V.A. (2004) The RNA interference proteins and vasa locus are involved in the silencing of retrotransposons in the female germline of Drosophila melanogaster. *RNA Biol.*, **1**, 54–58.

75. Gao,G., Walser,J.C., Beaucher,M.L., Morciano,P., Wesolowska,N., Chen,J. and Rong,Y.S. (2010) HipHop interacts with HOAP and HP1 to protect Drosophila telomeres in a sequence-independent manner. *EMBO J.*, **29**, 819–829.

76. Keller,C., Adaixo,R., Stunnenberg,R., Woolcock,K.J., Hiller,S. and Buhler,M. (2012) HP1(Swi6) mediates the recognition and destruction of heterochromatic RNA transcripts. *Mol. Cell*, **47**, 215–227.

77. Cotobal,C., Rodriguez-Lopez,M., Duncan,C., Hasan,A., Yamashita,A., Yamamoto,M., Bahler,J. and Mata,J. (2015) Role of Ccr4-Not complex in heterochromatin formation at meiotic genes and subtelomeres in fission yeast. *Epigenet. Chromatin*, **8**, 28.

78. Klenov,M.S., Lavrov,S.A., Stolyarenko,A.D., Ryazansky,S.S., Aravin,A.A., Tuschl,T. and Gvozdev,V.A. (2007) Repeat-associated siRNAs cause chromatin silencing of retrotransposons in the Drosophila melanogaster germline. *Nucleic Acids Res.*, **35**, 5430–5438.

79. Fischer,S.E., Pan,Q., Breen,P.C., Qi,Y., Shi,Z., Zhang,C. and Ruvkun,G. (2013) Multiple small RNA pathways regulate the silencing of repeated and foreign genes in C. elegans. *Genes Dev.*, **27**, 2678–2695.

80. Asif-Laidin,A., Delmarre,V., Laurentie,J., Miller,W.J., Ronsseray,S. and Teysset,L. (2017) Short and long-term evolutionary dynamics of subtelomeric piRNA clusters in Drosophila. *DNA Res.*, **24**, 459–472.

81. Luke,B., Panza,A., Redon,S., Iglesias,N., Li,Z. and Lingner,J. (2008) The Rat1p 5′ to 3′ exonuclease degrades telomeric repeat-containing RNA and promotes telomere elongation in Saccharomyces cerevisiae. *Mol. Cell*, **32**, 465–477.

82. Wagner,E., Clement,S.L. and Lykke-Andersen,J. (2007) An unconventional human Ccr4-Caf1 deadenylase complex in nuclear cajal bodies. *Mol. Cell Biol.*, **27**, 1686–1695.

83. Ilyin,A.A., Ryazansky,S.S., Doronin,S.A., Olenkina,O.M., Mikhaleva,E.A., Yakushev,E.Y., Abramov,Y.A., Belyakin,S.N., Ivankin,A.V., Pindyurin,A.V. *et al.* (2017) Piwi interacts with chromatin at nuclear pores and promiscuously binds nuclear transcripts in Drosophila ovarian somatic cells. *Nucleic Acids Res.*, **45**, 7666–7680.

84. Sugiyama,T., Thillainadesan,G., Chalamcharla,V.R., Meng,Z., Balachandran,V., Dhakshnamoorthy,J., Zhou,M. and Grewal,S.I.S. (2016) Enhancer of rudimentary cooperates with conserved RNA-Processing factors to promote meiotic mRNA decay and facultative heterochromatin assembly. *Mol. Cell*, **61**, 747–759.

85. Bronner,C., Salvi,L., Zocco,M., Ugolini,I. and Halic,M. (2017) Accumulation of RNA on chromatin disrupts heterochromatic silencing. *Genome Res.*, **27**, 1174–1183.

86. Assenholt,J., Mouaikel,J., Saguez,C., Rougemaille,M., Libri,D. and Jensen,T.H. (2011) Implication of Ccr4-Not complex function in mRNA quality control in Saccharomyces cerevisiae. *RNA*, **17**, 1788–1794.

87. Graham,A.C., Kiss,D.L. and Andrulis,E.D. (2006) Differential distribution of exosome subunits at the nuclear lamina and in cytoplasmic foci. *Mol. Biol. Cell*, **17**, 1399–1409.

88. Yamanaka,S., Mehta,S., Reyes-Turcu,F.E., Zhuang,F., Fuchs,R.T., Rong,Y., Robb,G.B. and Grewal,S.I. (2013) RNAi triggered by specialized machinery silences developmental genes and retrotransposons. *Nature*, **493**, 557–560.

89. Buhler,M., Haas,W., Gygi,S.P. and Moazed,D. (2007) RNAi-dependent and -independent RNA turnover mechanisms contribute to heterochromatic gene silencing. *Cell*, **129**, 707–721.